Earthquake Engineering, Tenth World Conference © 1992 Balkema, Rotterdam. ISBN 90 5410 060 5

Screening of surface waves by composite wave barriers

Elizabeth N. Its & Jong S. Lee
Clarkson University, USA

ABSTRACT: Propagation of surface waves across a vertical wave barrier with non-rigid contacts inserted between two homogeneous quarter-spaces is considered in this paper. An approximate analytical solution based on Green's function technique is developed to estimate the screening effect of the barrier. This mathematical model describes a composite barrier which consists of the combination of high and low velocity layers. The screening effectiveness of barriers with various elastic parameters and boundary conditions are compared and discussed in some details.

1 INTRODUCTION

Isolation of structures and machine foundations from ground-transmitted vibrations by installation of wave barriers has been attempted many times and has met with various degrees of success (Barkan 1962; Richart et al. 1970; Woods 1968). Many numerical and experimental investigations have confirmed the effectiveness of deep narrow open trenches for reducing the amplitude of the transmitted wave. Nevertheless, keeping trenches open for depths of practical concern can pose a serious problem from the engineering point of view. One way to overcome this difficulty is to use in-filled trenches. Successful application of bentonite-slurry filled trenches, for example, was reported by Dolling (1965). In the last three decades various numerical, experimental and analytical techniques have been applied to study the surface wave propagation across different types of barriers or in-filled trenches (e.g., Aboudi 1973; Segol et al. 1978; Leung et al. 1990; Ahmad and Al-Hussaini 1991). The application of approximate analytical techniques to study surface wave propagation in inhomogeneous media has been reviewed in detail in Knopoff and Hudson (1964), Its and Yanovskaya (1985) and Levshin et al. (1989).

Another way to achieve screening of surface waves without compromising the stability of soil is to employ a mixed type of barriers such as a combination of sheet pile wall and open or in-filled trench (Richart et al. 1970). An example of such combination was reported by McNeil et al. (1965). However, no numerical or analytical investigation on the composite barriers has been reported. The lack of analytical studies on this seemingly promising scheme for the wave screening is the direct motivation of this investigation.

In this paper the aproximate Green's function technique developed by Its and Yanovskaya (1985) is employed to estimate the effect of such combination by considering the model of non-rigid high velocity layer in a low velocity soil. This model describes the combination of high and low velocity obstacles. The former is modeled by differential matrix operators which are derived by using the Taylor's series expansion to relate the field quantities at each side of the layer. The latter ones are modeled by non-rigid (unwelded) contact conditions at both sides of the high velocity layer (Podypolsky 1963). Results of computation for combined obstacles are compared to separate high and low velocity obstacles. Dependence of the screening effect on various factors such as the non-rigidness parameter, width of the layer and incidence angle are examined. Advantages and disadvantages of different models are discussed in some details.

2 THE METHOD

Let a stationary Rayleigh wave be incident with the angle θ_1 to a narrow vertical layer inserted between two quarter-spaces denoted by indices 1 and 2 as shown in Fig. 1a. Material parameters of the quarter-spaces and the layer are $v_s^{(1)}$, $v_p^{(1)}$, $\rho^{(1)}$, $v_s^{(2)}$, $v_p^{(2)}$, $\rho^{(2)}$ and v_s, v_p, ρ, respectively, where $v_s^{(i)}$ and $v_p^{(i)}$ are the velocities of shear and compression wave, respectively, and $\rho^{(1)}$ is the density of the corresponding medium. The displacements and stresses of R waves in the medium 1 and 2 can be written as follows (Its and Yanovskaya

1985):

$$
\begin{aligned}
U^{(1)}(x,y,z) &= u^{(1)}(z)e^{i[\omega t - \xi^{(1)}(x\cos\theta_1 + y\sin\theta_1)]} \\
&\quad + \alpha\bar{u}^{(1)}(z)e^{i[\omega t + \xi^{(1)}(x\cos\theta_1 - y\sin\theta_1)]} \\
U^{(2)}(x,y,z) &= \beta u^{(2)}(z)e^{i[\omega t - \xi^{(2)}(x\cos\theta_2 + y\sin\theta_2)]} \\
T_x^{(1)}(x,y,z) &= \tau^{(1)}(z)e^{i(\omega t - \xi^{(1)}(x\cos\theta_1 + y\sin\theta_1))} \\
&\quad + \alpha\bar{\tau}^{(1)}(z)e^{i(\omega t + \xi^{(1)}(x\cos\theta_1 - y\sin\theta_1))} \\
T_x^{(2)}(x,y,z) &= \beta\tau^{(2)}e^{i(\omega t - \xi^{(2)}(x\cos\theta_2 + y\sin\theta_2))}
\end{aligned} \tag{1}
$$

where α and β are the unknown reflection and transmission coefficients, θ_2 is the transmission angle, $\xi^{(i)}$ is the wave number, and $u^{(i)}$ and $\tau^{(i)}$ are the eigenfunctions of the Rayleigh wave. The components of the eigenfunctions are given by

$$
\begin{aligned}
u_x^{(i)} &= \mp iu^{(i)}\cos\theta_i \\
u_y^{(i)} &= -iu^{(i)}\sin\theta_i \\
u_z^{(i)} &= w^{(i)} \\
\tau_x^{(i)} &= -(\lambda^{(i)} + 2\mu^{(i)})\xi^{(i)}u^{(i)} + 2\mu^{(i)}\xi^{(i)}u^{(i)}\sin^2\theta_i + \lambda^{(i)}\frac{\partial}{\partial z}w^{(i)} \\
\tau_y^{(i)} &= \mp \xi^{(i)}\mu^{(i)}u^{(i)}\sin 2\theta_i \\
\tau_z^{(i)} &= \mp i\mu^{(i)}\left(\frac{\partial}{\partial z}u^{(i)} + \xi^{(i)}w^{(i)}\right)\cos\theta_i
\end{aligned} \tag{2}
$$

where the upper sign corresponds to the incident and transmitted waves ($i = 1, 2$) and lower one to the reflected waves (marked by bar), $\lambda^{(i)}$ and $\mu^{(i)}$ are the Lame parameters. The eigenfunctions are assumed to be normalized according to

$$
\int_0^\infty (\tau^{(i)*}u^{(i)} - \tau^{(i)}u^{(i)*})dz = \pm 2i\cos\theta_i \ . \tag{3}
$$

Now we assume that the layer is in non-rigid contact with the host media and that a coupling between surface and body waves which can arise in the vicinity of the layer is negligible. In this case stresses and normal components of displacement are continuous at the both vertical boundaries and there is a partial sliding along the boundaries proportional to tangential components of the stresses (Podypolsky 1965) such that

$$
\begin{aligned}
U_n^{(1)}(0,y,z) &= U_n(0,y,z) \\
T_x^{(1)}(0,y,z) &= T_x(0,y,z) \\
U_t^{(1)}(0,y,z) + mT_{xt}^{(1)}(0,y,z) &= U_t(0,y,z) \\
U_n^{(2)}(h,y,z) &= U_n(h,y,z) \\
T_x^{(2)}(0,y,z) &= T_x(0,y,z) \\
U_t(h,y,z) + mT_{xt}(h,y,z) &= U_t^{(2)}(h,y,z)
\end{aligned} \tag{4}
$$

where U and T are the displacement and the stress within the layer and m is the so-called non-rigid parameter defined by

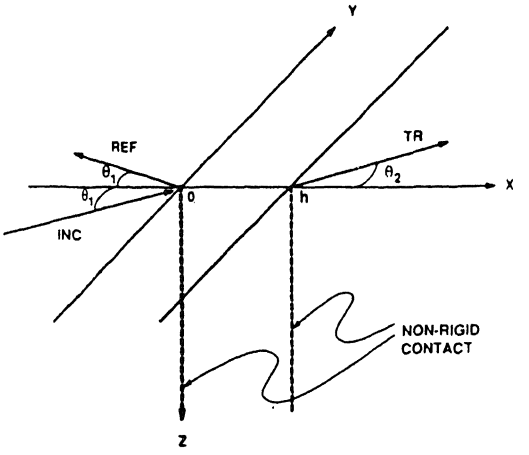

Fig. 1a. The model of non-rigid layer.

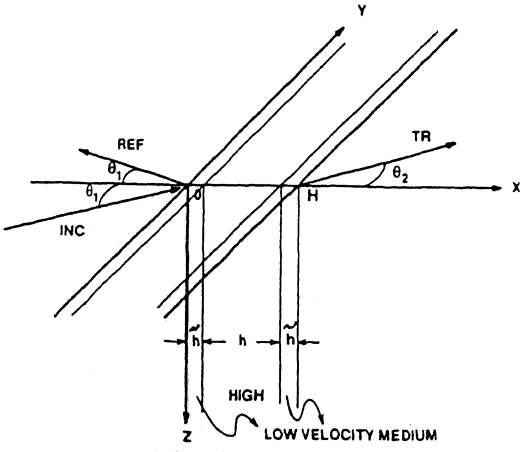

Fig. 1b. Physical equivalence of the model

$$
m = \lim\frac{\tilde{h}}{\tilde{\mu}} \qquad \tilde{h} \to 0, \quad \tilde{\mu} \to 0 \tag{5}
$$

where $\tilde{h}$ and $\tilde{\mu}$ are the width and the shear modulus of a low velocity layer between the host medium and the high velocity layer, respectively (see Fig. 1b). For a narrow low velocity layer, i.e., $\tilde{h} \ll l$ (l = wavelength) $\tilde{\mu} \ll \mu^{(i)}$ or μ, m can be determined by

$$
m = \frac{\tilde{h}}{\tilde{\mu}}. \tag{6}
$$

The displacement and stress U and T in (4) cannot be expressed in analytical form. One can eliminate them by expanding U and T into Taylor's series with respect to x in the small vicinity of $x=0$ and $x=h$. The decomposition of x component of displacement U can be written as

$$U_x(h,y,z)=U_x(0,y,z)+h\frac{\partial}{\partial x}U_x+\frac{h^2}{2}\frac{\partial^2}{\partial^2 x}U_x \qquad (7)$$

Here we employ the quadratic approximation of Taylor's series. Advantages of the second order approximation compared to a linear one was discussed in Its (1991). The Hooke relations and the equation of motion in the layer can be used to transform the first and second derivatives of the displacement. The former ones have the form:

$$\begin{aligned} T_{xx} &= (\lambda+2\mu)\frac{\partial}{\partial x}U_x+\lambda\frac{\partial}{\partial y}U_y+\lambda\frac{\partial}{\partial z}U_z \\ T_{xy} &= \mu(\frac{\partial}{\partial x}U_y+\frac{\partial}{\partial y}U_x) \\ T_{xz} &= \mu(\frac{\partial}{\partial z}U_x+\frac{\partial}{\partial x}U_z) \end{aligned} \qquad (8)$$

Therefore, the first derivative can be expressed as

$$\frac{\partial}{\partial x}U_x=\frac{T_{xx}}{\lambda+2\mu}-\frac{\lambda}{\lambda+2\mu}(\frac{\partial}{\partial y}U_y+\frac{\partial}{\partial z}U_z) \qquad (9)$$

Taking into account the boundary conditions (4) we can rewrite the above relationship as

$$\begin{aligned} \frac{\partial}{\partial x}U_x=\frac{T_{xx}^{(1)}}{\lambda+2\mu}&-\frac{\lambda}{\lambda+2\mu}\frac{\partial}{\partial y}(U_y^{(1)}+mT_{xy}^{(1)}) \\ &-\frac{\lambda}{\lambda+2\mu}\frac{\partial}{\partial z}(U_z^{(1)}+mT_{xz}^{(1)}) \end{aligned} \qquad (10)$$

Using the equation of motion for the x component,

$$-\rho\omega^2U_x=\frac{\partial}{\partial x}T_{xx}+\frac{\partial}{\partial y}T_{xy}+\frac{\partial}{\partial z}T_{xz} \qquad (11)$$

and equations (4) and (8), the second derivative can be expressed as the following:

$$\begin{aligned} \frac{\partial^2}{\partial^2 x}U_x=\frac{1}{\lambda+2\mu}\Big[&-\rho\omega^2U_x^{(1)}-\frac{\partial}{\partial y}T_{xy}^{(1)}-\frac{\partial}{\partial z}T_{xz}^{(1)} \\ &-\lambda\frac{\partial}{\partial y}\frac{1}{\mu}(T_{xy}^{(1)}-\mu\frac{\partial}{\partial y}U_x^{(1)}) \\ &-\lambda\frac{\partial}{\partial z}\frac{1}{\mu}(T_{xz}^{(1)}-\mu\frac{\partial}{\partial z}U_x^{(1)})\Big] \end{aligned} \qquad (12)$$

In writing above, we assumed that elastic parameters are laterally homogeneous throughout the layer. Finally, combining (10) and (12), equation (7) can be written as

$$\begin{aligned} U_x^{(2)}=U_x^{(1)}+\frac{h}{\lambda+2\mu}\Big[&T_{xx}^{(1)}-\frac{\lambda}{\lambda+2\mu}\frac{\partial}{\partial y}(U_y^{(1)}+mT_{xy}^{(1)})- \\ &\frac{\lambda}{\lambda+2\mu}\frac{\partial}{\partial z}(U_z^{(1)}+mT_{xz}^{(1)})\Big] \end{aligned}$$

$$\begin{aligned} &+\frac{h^2}{2(\lambda+2\mu)}\Big[-\rho\omega^2U_x^{(1)}-\frac{\partial}{\partial y}T_{xy}^{(1)}- \\ &\lambda\frac{\partial}{\partial y}\frac{1}{\mu}(T_{xy}^{(1)}-\mu\frac{\partial}{\partial y}U_x^{(1)})-\lambda\frac{\partial}{\partial z}\frac{1}{\mu}(T_{xz}^{(1)}-\mu\frac{\partial}{\partial z}U_x^{(1)})\Big] \end{aligned} \qquad (13)$$

Similar relationships can be obtained for the other components of displacement and stress and can be cast in the matrix form as follows:

$$\begin{aligned} \mathbf{U}^{(2)}(h,y,z) &= \mathbf{Q}^{(U)}\mathbf{R}^{(1)}(0,y,z)+m\,\mathbf{T}_{xl}^{(2)}(h,y,z) \\ \mathbf{T}_x^{(2)}(h,y,z) &= \mathbf{Q}^{(T)}\mathbf{R}^{(1)}(0,y,z) \\ \mathbf{U}^{(1)}(0,y,z) &= \overline{\mathbf{Q}}^{(U)}\mathbf{R}^{(2)}(h,y,z)-m\,\mathbf{T}_{xl}^{(1)}(0,y,z) \\ \mathbf{T}_x^{(1)}(0,y,z) &= \overline{\mathbf{Q}}^{(T)}\mathbf{R}^{(2)}(h,y,z) \end{aligned} \qquad (14)$$

where vectors $\mathbf{R}^{(1)}$ and $\mathbf{R}^{(2)}$ are defined by

$$\mathbf{R}^{(1)}=\begin{bmatrix}\mathbf{U}^{(1)}+m\,\mathbf{T}_{xl}^{(1)}\\ \mathbf{T}_x^{(1)}\end{bmatrix} \qquad \mathbf{R}^{(2)}=\begin{bmatrix}\mathbf{U}^{(2)}-m\,\mathbf{T}_{xl}^{(2)}\\ \mathbf{T}_x^{(2)}\end{bmatrix} \qquad (15)$$

Complete expressions for the matrix operators $\mathbf{Q}^{(U)}$ and $\mathbf{Q}^{(T)}$ are given in Its and Lee (1992) Operators $\overline{\mathbf{Q}}^{(U)}$ and $\overline{\mathbf{Q}}^{(T)}$ connecting the fields in the medium 1 and 2 can be obtained from $\mathbf{Q}^{(U)}$ and $\mathbf{Q}^{(T)}$ by replacing h with $-h$. The relationships (14) are to be used for determination of reflected and transmitted wave fields at the boundaries of the layer.

By introducing the vectors $\mathbf{r}^{(1)}$ and $\mathbf{r}^{(2)}$ as

$$\mathbf{r}^{(1)}=\begin{bmatrix}\mathbf{u}^{(1)}+m\tau_l^{(1)}\\ \tau^{(1)}\end{bmatrix} \qquad \mathbf{r}^{(2)}=\begin{bmatrix}\mathbf{u}^{(2)}-m\tau_l^{(2)}\\ \tau^{(2)}\end{bmatrix}$$

$$\mathbf{r}^{(1)}=\begin{bmatrix}\overline{\mathbf{u}}^{(1)}-m\overline{\tau}_l^{(1)}\\ \overline{\tau}^{(1)}\end{bmatrix} \qquad (16)$$

we rewrite displacements of the reflected wave in the form

$$\begin{aligned} \mathbf{U}^{ref}(0,y,z)=\beta\overline{\mathbf{Q}}^{(U)}\mathbf{r}^{(2)}(z)\,e^{-i\xi^{(2)}(h\cos\Theta_2+y\sin\Theta_2)} \\ -\mathbf{u}^{(1)}(z)e^{-i\xi^{(1)}y\sin\theta_1}-m\tau_l^{(1)}\,e^{-i\xi^{(1)}y\sin\theta_1} \\ -m\alpha\overline{\tau}_l^{(1)}\,e^{-i\xi^{(1)}y\sin\theta_1} \end{aligned} \qquad (17)$$

Similar expressions can be written for other fields.

The Green function technique developed in Its and Yanovskaya (1985) and Its (1991) is employed then to determine the reflection and transmission coefficients of Rayleigh waves across the layer. In accordance with this technique the displacement at any point of the media 1 and 2 can then be determined by the value of field at the boundary by the use of the representation theorem:

$$(U^{ref}(x_1,y_1,z_1),\mathrm{I}) =$$

$$\int_0^\infty\int_{-\infty}^\infty [G_1^l(x_1,y_1,z_1,0,y,z)T_x^{ref} - P(G_1^l)U^{ref}(0,y,z)]dydz$$

$$(U^{tr}(x_2,y_2,z_2),\mathrm{I}) = \tag{18}$$

$$\int_0^\infty\int_{-\infty}^\infty [G_2^l(x_2,y_2,z_2,h,y,z)T_x^{tr} - P(G_2^l)U^{tr}(h,y,z)]dydz$$

where G_i^l and $P(G_i^l)$ are the Green function for surface waves and the corresponding stresses for half-space with parameters of the ith medium, respectively (Aki and Richards 1980). Equations (14) and (18) are the complete system for the estimation of reflection and transmission coefficients of surface waves. We first insert reflected and transmitted fields of the form (17) into (18) with far field Green's functions and then integrate the resulting expressions over y by using the stationary phase method. Finally we obtain a system of equations for the estimation of reflection and transmission coefficients as follows:

$$a(\cos\theta_1 - Z^{(3)}) = be^{-i\xi^{(2)}h\cos\theta_2}Z^{(1)} + Z^{(2)} \tag{19}$$

$$b(\cos\theta_2 - Z^{(6)}) = -e^{i\xi^{(2)}h\cos\theta_2}Z^{(4)} - e^{i\xi^{(2)}h\cos\theta_2}aZ^{(5)}$$

where

$$Z^{(1)} = \frac{1}{2i}\int_0^\infty (\overline{K}^{(T)}r^{(2)}\overline{u}^{(1)*} - \overline{K}^{(U)}r^{(2)}\overline{\tau}^{(1)*})dz$$

$$Z^{(2)} = \frac{1}{2i}m\int_0^\infty \tau_t^{(1)}\overline{\tau}_t^{(1)*}\,dz$$

$$Z^{(3)} = \frac{1}{2i}m\int_0^\infty \overline{\tau}_t^{(1)}\overline{\tau}_t^{(1)*}\,dz \tag{20}$$

$$Z^{(4)} = \frac{1}{2i}\int_0^\infty (K^{(T)}r^{(1)}u^{(2)*} - K^{(U)}r^{(1)}\tau^{(2)*})dz$$

$$Z^{(5)} = \frac{1}{2i}\int_0^\infty (K^{(T)}\overline{r}^{(1)}u^{(2)*} - K^{(U)}\overline{r}^{(1)}\tau^{(2)})dz$$

$$Z^{(6)} = \frac{1}{2i}m\int_0^\infty \tau_t^{(2)}\tau_t^{(2)*}\,dz$$

where the matrices $K^{(T)}$, $K^{(U)}$, $\overline{K}^{(T)}$, and $\overline{K}^{(U)}$ may be obtained from the matrices $Q^{(T)}$, $Q^{(U)}$, $\overline{Q}^{(U)}$, and $\overline{Q}^{(T)}$, respectively, by replacing $\partial/\partial y$ with $-\xi^{(i)}\sin\theta_i$. The system of equations (19) and (20) can be used for the estimation of reflection and transmission coefficients of Rayleigh waves at an infinite vertical layer with non-rigid contacts.

3 RESULTS AND DISCUSSIONS

The Green's function technique described in the previous section is employed here to calculate reflection and transmission coefficients due to the propagation of Rayleigh wave across a vertical layer inserted between two homogeneous quarter-spaces. In all calculations we used the ratio of the reflection coefficient to the transmission coefficient, which will be referred as screen parameter $\gamma = |\alpha|/|\beta|$, to describe the screening effect of the wave barrier. In what follows results of computation are presented and discussions are made:

3.1 Elastic parameters and boundary conditions

In order to study the effect of elastic properties of the obstacle and boundary conditions on the screen parameter three models were considered first: a high and low velocity layer with rigid contact and a high velocity layer with non-rigid contact. Three generic materials - sand, concrete and bentonite-slurry - are chosen to describe the host medium, high velocity material and low velocity material respectively. The elastic parameters of each medium are given in Table 1. The total width of obstacles under consideration was chosen at $H=0.1l$. Fig. 2 shows the screen parameter γ as a function of the incident angle θ_1 for three different models of obstacles. It is shown in the figure that for the same width and the similar material contrast (with respect to shear velocity) the screening effect of the low velocity layer (curve 1) is bigger than that of the high velocity layer (curve 2) for small angles of incidence. At the same time we can see a significant increase of the screen parameter for the high velocity obstacle and a decrease for the low velocity obstacle as the incident angle is increased. It is noted that there exists a sharp minimum of screen parameter in the vicinity of 60 degrees for the low velocity obstacle. After the minimum γ increases very sharply with the incident angle. It should be noted that it is impossible to consider the propagation across the layer as a consistent Rayleigh wave propagation across the two boundaries since in the narrow layer between the two boundaries there exists a very complex interference. It is obvious, however, that the right-hand-side boundary plays less significant role on the propagation because some part of the energy reflects at the left boundary. At the same time the effect of L-H (low velocity to high velocity medium) boundary is more important than H-L boundary for propagation for large angles of incidence because of the critical reflection. Therefore, one may suppose that for the high velocity layer effect of the first and more powerful boundary leads to a sharp increase of screen parameter for large angles. For low velocity layer effect of critical reflection at second boundary also begins to play the same role, but this effect is weaker because of the energy loss at the first boundary, so even for identical contrast the curve 1 will lay under the curve 2 for large angles of incidence. The third curve in Fig. 2 corresponds to layer with non-rigid contact. By this non-rigid layer we model the composite barrier with the same total width $H = 0.1l$. This composite barrier consists of three layers; that is, a high velocity layer ($h = 0.05l$) is

Table 1. Elastic parameters

Medium	$\rho(g/cm^3)$	$v_s(km/scc)$	$v_p(km/scc)$
soil	2.0	0.5	2.0
concrete	2.4	1.35	2.38
bentonite -slurry	1.8	0.2	2.0

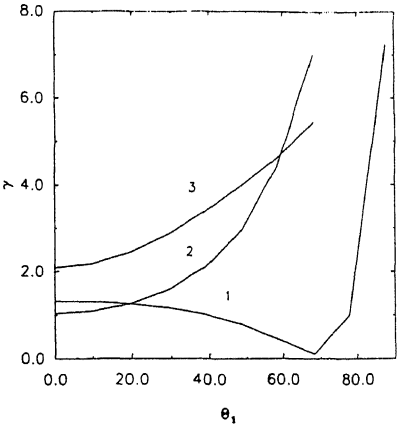

Fig. 2. Screen parameter γ as a function of an angle of incidence θ_1 for (1) low velocity rigid layer, (2) high velocity rigid layer and (3) high velocity non-rigid layer.

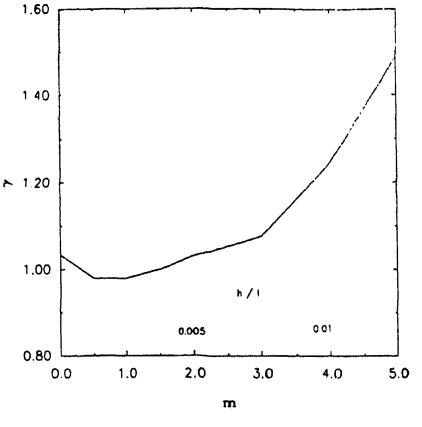

Fig. 3. Screen parameter γ for a composite barrier as a function of the non-rigid parameter m.

now sandwiched between two low velocity layers ($\tilde{h} = 0.025l$). It is shown in the figure that this composite barrier gives higher screening than the low velocity one, and the screen ratio does not decrease as the incident angle increases; therefore, high velocity layer with non-rigid contacts as a screen has the advantage of high velocity obstacle for big angle of incidence and gives higher level of screening compared to low velocity obstacle for relatively small angles of incidence.

3.2 Non-rigid parameter

Influence of the non-rigidness parameter m on the screen parameter γ was examined next. It was shown (Levshin et al. 1989) that even a small increase of the non-rigidness of the boundary resulted in a significant increase of reflection (or decrease of the transmission) of a Rayleigh wave. We expected to get a similar result for the layer with non-rigid contact. To validate this assumption we computed the screen parameter of the high velocity layer with non-rigid contact for normal incidence of wave for varying values of non-rigidness parameter. Nevertheless, results of computation did not completely confirm our assumption. The results of computation are given in Fig 3 for normal incidence of Rayleigh wave to the layer with width h=0.1l. Parameters of the layer and host medium are the same as in Table 1. One can see that for variation of m (which we interpreted as a variation of low velocity layer width $\tilde{h}/l$ for a fixed ratio of shear moduli $\tilde{\mu}/\mu$ =1/7) screen parameter decreases with an increase in $\tilde{h}/l$ for very narrow low velocity layers compared to a high velocity layer with rigid contact. A further increase of $\tilde{h}/l$ results in an increase in the screen parameter in the interval under consideration. This result may be explained as the following: for small width of low velocity layers the wave does not feel them separately from high velocity obstacle, but as a little smoothing boundaries of high velocity layer. As a result, the screen parameter becomes smaller than for sharp boundaries. As the width of the low velocity layer increases, the effect of all sharp boundaries becomes significant, and this leads to a steady increase of the screen parameter. This interpretation seems to be reasonable since we model the low velocity layers by the non-rigid contact where only $m=h/\mu$ (but not $\tilde{h}$ and $\tilde{\mu}$ separately) is fixed.

4 CONCLUSION

An approximate analytical technique based on the Green's function method is developed to study Rayleigh wave propagation across a composite (high and low velocity) wave barrier. The barrier is modeled as a high velocity layer with non-rigid (unwelded) contacts inserted between horizontally homogeneous

quarter-spaces. Relations connecting the displacements and stresses at two opposite boundaries of the layer in the form of matrix operators are derived by using Taylor's series decomposition of the field in the layer. Results of calculation for barriers with various parameters are presented. It is shown that the composite barrier can give a significant improvement in screening surface waves over the performance of a barrier with a single high or low velocity layer.

REFERENCES

Aboudi, J. 1973. Elastic waves in half-space with thin barrier. J. Eng. Mech. Div., ASCE, EM1: 69-83.

Ahmad, S. & Al-Hussaini, T.M. 1991. Simplified design for vibration screening by open and in-filled trenches, J. Geotech. Eng., 117(1): 67-87.

Aki, K. & Richards, P.G. 1980. Quantitative Seismology, Freeman, San-Francisco.

Barkan, D.D. 1962. Dynamics of Bases and Foundations. McGraw-Hill, New York.

Dolling, H.J. 1965. Schwingunsisolierung von Bauwerkendurch tiefe, auf geeignete weise stabilisierte Schiltze, Sonderdruck aus VDI - Berichte 88:3741.

Hudson, J.A. & Knopoff, L. 1964. Transmission and reflection of surface waves at a corner, J. Geophys. Res. 69: 281.

Its, E.N. & Yanovskaya, T.B. 1985. Propagation of surface waves in half-space with vertical, inclined or curved interspaces, Wave motion , 7: 79-94.

Its, E.N. 1991. Surface wave propagation across a narrow vertical layer between horizontally homogeneous quarter-spaces. Wave Motion, 14: 11-23.

Its, E.N. & Lee, J.S. Surface waves of oblique incidence across in-filled trenches. J. Eng. Mech. (under review).

Leung, K.L., Beskos, D.E. & Vardoulakis, I.G. 1990. Vibration isolation using open or filled trenches. Computational Mechanics, 7: 137-148.

Levshin, A.L. et al. 1989. Seismic Surface Waves in Horizontally Inhomogeneous Earth, Elsevier Sci. Pub., Netherlands.

McNeill, R.L., Margason, B.E. and Bobcock, F.M. 1965. The role of soil dynamics in the design of stable test pads, Guidance and Control Conference, Minneapolis, Minn., Aug. 16-18.

Podypolsky, B.P. 1963. Reflection and transmission of P-waves at the non-rigid contact of elastic media, ISSN Geophys., 4: 525-531 (in Russian).

Richart, F.E., Jr. et al. 1970. Vibrations of Soils and Foundations, Prentice-Hall, Englewood Cliff, NJ.

Segol, G., Lee, P.C .Y. & Abel, J.F. 1978. Amplitude reduction of surface waves by trenches, J. Eng. Mech. Div., EM3: 621-641.

Sicharulidze, D.I. et al. 1988. The Surface Waves in the Inverse Problem of Seismology, Erevan (in Russian).

Woods, R.D. 1968. Screening of surface waves in soils. J. Soil Mech and Found. Div., Proc. ASCE, 94(4): 951-979.